

Synthesis and Characterization of Molecularly Imprinted Polymer for the Removal/Extraction of Thymol from Spiked Blood Serum and River water

SALMA BAKHTIAR, SHOWKAT AHMAD BHAWANI* and SYED RIZWAN SHAFQAT

Department of Chemistry, Faculty of Resource Science and Technology, Universiti Malaysia Sarawak (UNIMAS), Kuching 94300, Malaysia

*Corresponding author: E-mail: sabhawani@gmail.com

Received: 25 April 2019;

Accepted: 1 June 2019;

Published online: 28 September 2019;

AJC-19573

Molecularly imprinted polymers (MIPs) were prepared by precipitation polymerization using thymol as a template molecule, acrylamide as a functional monomer and N,N-methylbisacrylamide as the crosslinker with a non-covalent approach. The polymers were characterized by scanning electron microscopy (SEM), energy-dispersive X-ray spectroscopy (EDX), fourier-transform infra red spectroscopy (FT-IR) and Brunauer-Emmett-Teller (BET). The SEM results depicted that the shape of polymer particles is spherical with uniform size (micrometers). The BET results also showed better surface area, pore size and pore volume of MIP as compared to non-imprinted polymer (NIP). A series of parameters such as initial concentration, polymer dosage, effect of pH and selectivity with structural analogue were conducted. The selectivity of MIP towards thymol was appreciable as compared to its structural analogue gallic acid with a relative selectivity coefficient of 3.59. Finally, MIP has been successfully used for extraction of thymol from the spiked blood serum (84 %) and river water sample (98 %).

Keywords: Thymol, Molecularly imprinted polymers, Extraction, Blood serum, River water.

INTRODUCTION

Thymol (5-methyl-2-(methyl ethyl)phenol), a constituent of oil of thyme, a naturally occurring mixture of compounds in the plant (*Thymus vulgaris* L., or thyme) [1]. It is an active ingredient in pesticide products for animal repellent, fungicide, medical disinfectant, tuberculocide and virucide. Thymol has also many non-pesticidal uses, such as in perfumes, mouth washes, food flavouring, pharmaceutical preparations, cosmetics and also as a stabilizer to several therapeutic agents, including halothane [2,3]. Thymol is widely used in the chemical industry to stabilize and to store solutions and serum samples [4]. Thymol resembles phenol in its action, but owing to its insolubility in body fluids, its absorption is much more slow and less irritant to wounds, while its germicidal action is greater than that of phenol but less than that of naphthol. Thymol is considered as a mild irritant and less toxic but it can also cause gastric pain, nausea, vomiting, central hyperactivity, etc. in human beings. The continuous disposal of thymol in the environment may also cause harmful effects to the aquatic life. Therefore,

monitoring of thymol is very important in both biological and environmental samples.

A number of analytical methods have been reported for the determination of thymol, such as HPLC [5-10], LC with electrochemical detection [11], gas chromatography [12-18], differential pulse voltammetry [19], spectrometry [20,21], colorimetric analysis [22], TLC [23,24] and flow injection spectrophotometry [25]. However, some of these methods are expensive, time consuming and/or require several tedious conditions. In this work, a rapid and sensitive method using molecularly imprinted polymers was proposed for the determination of thymol in environmental and biological samples. This technique is safe, simple, fast and accurate and has been satisfactorily applied to the extraction/removal of thymol in river water and human blood serum.

Molecular imprinting is a technology that facilitates the production of artificial receptors towards compounds of interest [26]. Molecularly imprinted polymers (MIPs) are porous materials with specific binding cavities for recognition of a particular target molecule. Molecularly imprinted polymers have many

advantages such as high selectivity, mechanical strength and chemical inertness, low cost ease of preparation, and a long storage life span. Over the past decades, these polymers have been successfully used in different fields such as chemical sensors, enzyme mimicking, catalysis, intelligent drug delivery, *etc.* [27]. MIPs have been used for the separation of isomers and enantiomers, in solid-phase extraction, in biochemical sensors and chemosensors, in simulating enzyme-catalyzed pharmaceutical analysis, in sorbents and in membrane separation technologies. MIPs are prepared in different configurations including polymer beads, polymer monoliths and polymers membranes. Further, MIPs are stable, easy to prepare, and inexpensive [28]. The current study investigates the potential of precipitation polymerization as a promising technique for the synthesis of imprinted materials for the extraction of thymol.

EXPERIMENTAL

Thymol was purchased from Sigma-Aldrich, 2,2'-azobis(isobutyronitrile) (AIBN) from R & M Marketing Company (U.K.), acetonitrile from Avantor Performance Materials Incorporated (USA), acrylamide, N,N-methylbisacrylamide (NNMB) and gallic acid were procured from Sigma-Aldrich. All the chemicals purchased were of analytical grade.

Synthesis of MIP and NIP: Molecularly imprinted polymers were synthesized using precipitation polymerization according to the molar ratios as listed in Table-1. For the preparation of thymol-imprinted polymer, thymol was dissolved in 50 mL of acetonitrile in a 250 mL conical flask, after that the functional monomer (acrylamide) was added. The whole mixture was sonicated for 5 min to get a homogenous solution. In separate flask a crosslinker N,N-methylbisacrylamide (NNMB) was dissolved in 25 mL DMSO and the solution was sonicated again for 5 min to disperse the cross-linker homogeneously. After that both the solutions were mixed in one flask and sonicated for 15 min. The reaction mixture was then purged with nitrogen gas for 15 min in order to prevent oxygen annihilation and was sealed under nitrogen. The reaction vessel was inserted in pre-heated water bath at 60 °C for 4 h. The temperature was increased from 60 to 80 °C for 2 h with a total polymerization time of 6 h. After the polymerization, the polymer particles were separated by filtration. The non-molecularly imprinted polymer (NIP) was prepared in the same way, but without thymol.

The template from polymer matrix was leached out from the imprinted polymer particles by washing with the mixture of methanol/acetic acid (90:10, v/v), until no template could be detected from the washing solvent by HPLC at 290 nm. The polymer particles were finally washed with acetone to remove

TABLE-1
COMPOSITION OF IMPRINTED AND
NON-IMPRINTED POLYMERS

Polymer	Template (Thymol, mmol)	Monomer (acrylamide, mmol)	Cross-linker (NNMB)	Molar ratio
MIP 1	1	3	16	1:3:16
MIP 2	1	4	16	1:4:16
MIP 3	1	5	16	1: 5:16
NIP	–	5	16	0:5:16

the acid residues, and the resulted imprinted polymers were dried at 60 °C for 6 h.

Fourier transform infrared spectra (4000-400 cm⁻¹) of MIPs and NIP were recorded in a neat and clean transparent KBr pellet. The morphologies of MIP and NIP were determined by SEM (JEOL JSM 6930 LA). The dried MIP particles were coated with gold before the SEM analysis.

Batch binding experiments: The 100 mg of MIP (MIP 1, MIP2, MIP3) particles were added to a series of conical flasks and labelled as MIP1, MIP2, MIP3 and NIP1 containing 10 mL of 20 ppm thymol solution at room temperature (27 °C). After that all conical flasks were shaken on a shaker at 250 rpm for 300 min. The samples were collected at different time intervals (0, 30, 60, 90, 120, 150, 180, 210, 240, 270 and 300 min). The collected samples were then analyzed by HPLC. HPLC was performed by using methanol acetonitrile and water (80:10:10, v/v/v, respectively) as a mobile phase and C₁₈ column as a stationary phase. The flow rate of sample was set at 0.5 mL/min and wavelength for analysis was 290 nm. The extraction percentage (%) of imprinted polymers (MIPs) and non-imprinted polymer (NIP) was calculated by the following equation:

$$\text{Extraction (\%)} = \frac{C_i - C_f}{C_i} \times 100 \quad (1)$$

where C_i and C_f are the initial and final concentration of thymol, respectively.

The other parameters like initial concentration, polymer dosage, pH and agitation rate were analyzed by changing one parameter and the other parameters were kept constant. All the optimized parameters are summarized in Table-2.

Selectivity test: In this experiment, recognition selectivity of synthesized MIP and NIP towards thymol was examined in the presence of competitive template. For this purpose, gallic acid was selected as a competitive template because it is a structural analog to thymol. The procedure included the mixing of equal proportion of both the templates. After that resulting mixture was added in the flask containing selected MIP. Same procedure

TABLE-2
DIFFERENT ADSORPTION PARAMETERS OF MIP FOR THE REMOVAL/EXTRACTION OF THYMOL

Parameters	Variation in parameter	Constant parameters
Different initial concentrations	10, 15, 20, 25, 30 ppm	Temperature 300 K, Agitation speed 250 rpm, Contact time 90 min, Adsorbent dose 300 mg, pH 7
Different dosage	100, 200, 300, 400, 500 mg	Temperature 300 K, Agitation speed 250 rpm, Contact time 90 min, pH 7, Concentration 20 ppm
pH	2, 5, 7, 10, 12	Temperature 300 K, Agitation speed 250 rpm, Contact time 90 min, Adsorbent dose 300 mg, Concentration 20 ppm.
Agitation rate	100, 150, 200, 250, 300 rpm	Temperature 300 K, Contact time 90 min, Adsorbent dose 300 mg, Concentration 20 ppm.

was followed for NIP. The adsorption capacity of the template or the competition spices was calculated using eqn. 1 [29]. The distribution coefficient was calculated according to eqn. 2:

$$K_D = \frac{Q_e}{C_e} \quad (2)$$

where K_D represents the distribution coefficient (L/g), Q_e (mg/g) is the equilibrium binding capacity, and C_e (mg/L) is the equilibrium concentration.

The selectivity coefficient for thymol with respect to the competition species gallic acid is calculated according to eqn. 3:

$$\alpha = \frac{K_{Dj}}{K_{Di}} \quad (3)$$

where α is the selectivity coefficient, i and j represent the template and competitor species, respectively. The value of α allows an evaluation of selectivity of MIP for thymol.

The relative selectivity coefficient (β) was also calculated according to eqn. 4

$$\beta = \frac{\alpha(\text{MIP})}{\alpha(\text{NIP})} \quad (4)$$

Extraction/removal of thymol from blood serum and river water: About 10 mL of drug-free fresh human blood was collected and then the whole blood was allowed to clot by leaving it undisturbed for 30 min at room temperature. After that the clotted blood was centrifuged at 5000 rpm for 15 min. The supernatant collected is the serum. After that blood serum was diluted with ultra-pure water in the ratio of 1:10. Next, 5 mL of diluted blood serum was spiked with 5 mL of 20 $\mu\text{g}/\text{mL}$ thymol. On the other hand, river water was filtered by using gravitational filtration to remove any suspended particles. Then, the presence of thymol in the collected river water was observed by using RP-HPLC. Then, thymol was spiked in river water with a total concentration of 20 $\mu\text{g}/\text{mL}$. About 100 mg of selected MIP and NIP were added into conical flasks containing 10 mL spiked blood serum and river water. The flask containing the whole mixture was agitated on a shaker for 90 min. The supernatant solution was collected after filtering the whole mixture. The extraction efficiency was evaluated by using eqn 1.

RESULTS AND DISCUSSION

Characterization of MIP: The FTIR spectra of MIPs and NIP are depicted in Fig. 1. A broad OH stretching peak appeared at 3343.24-3331.51 cm^{-1} and CH stretching at 2976.50-2972.32 cm^{-1} were observed in the spectra of MIPs. For NIP, OH stretching peak appeared at 3427.20 cm^{-1} and the N-H stretching vibration occurs at 2930.05 cm^{-1} . The C-N stretching absorption occurs in the 1384 cm^{-1} region. While, C=O stretching vibrations was observed in the 1656-1653 cm^{-1} range, which shows a strong ketone group band. Primary amides give other bending bands and a broad band around 716 cm^{-1} . A C-N stretching band appears at about 1429 cm^{-1} for acrylamide. The peaks around 874.33-878.72 cm^{-1} showed the =CH bending of vinyl group from monomer or cross-linker. There is a clear distinction in the shift of peaks for -OH and C=O stretching in the MIP3 and its NIP. This indicated the interaction of template with the monomer.

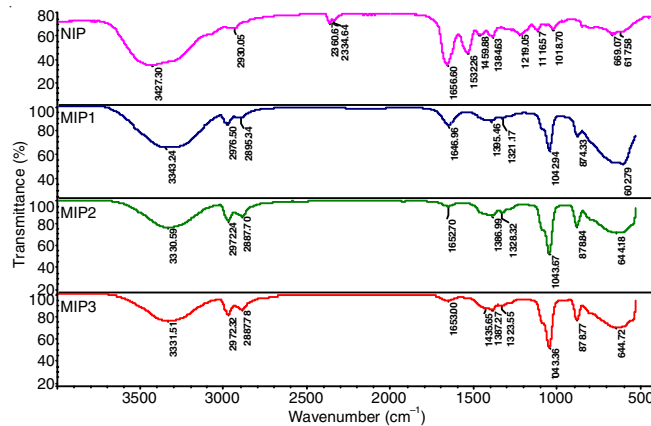


Fig. 1. FTIR of MIPs and NIP

SEM analysis: SEM micrographs of MIP and NIP particles are shown in Fig. 2a-b. From SEM images, it was found that a uniformly sized and spherical particles were obtained by precipitation polymerization. The choice of the reaction solvent and polymerization method are critical for the synthesis of uniformly microspheres and nanospheres [30]. In this research, polymers have been synthesized by precipitation polymerization method. This has been reported that the precipitation polymerization produces polymer particles with uniform shape and size [31-33]. The size of MIP particles was smaller than the corresponding NIP particles but there were not considerable differences in the morphology of imprinted and non-imprinted microspheres. These results led to this conclusion that the presence of template had a major effect on the size of the imprinted particles (MIP). The particle size differences between MIP and NIP may be due to molecular interaction between acrylamide and thymol. In the absence of template, functional monomer can form hydrogen-bonded dimers in the non-imprinting system, and the pre-polymerization solution contains both functional monomer dimers and free functional monomer. In the imprinting system, there are additional molecular interactions between functional monomer and template, which might somehow affect the growth of the cross-linked polymer nuclei [34].

Energy-dispersive X-ray spectroscopy (EDX): The EDX results show that MIP contains 89.49 % of carbon and 10.28 % of oxygen which is a good agreement with the theoretical formula percentage values (Fig. 3). This indicated that the backbone of polymer is mainly composed of carbon atoms.

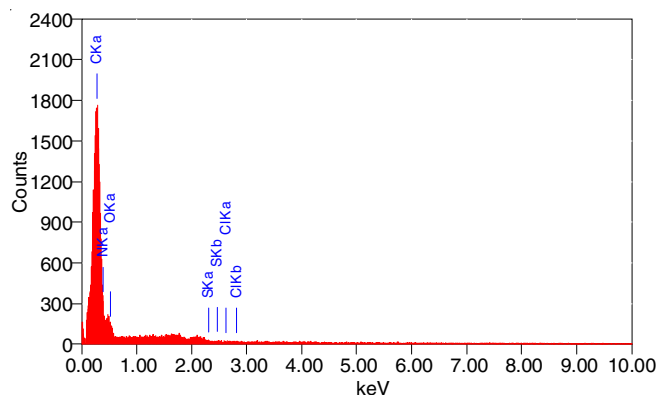


Fig. 3. Energy-dispersive X-ray spectroscopy (EDX) results of MIP

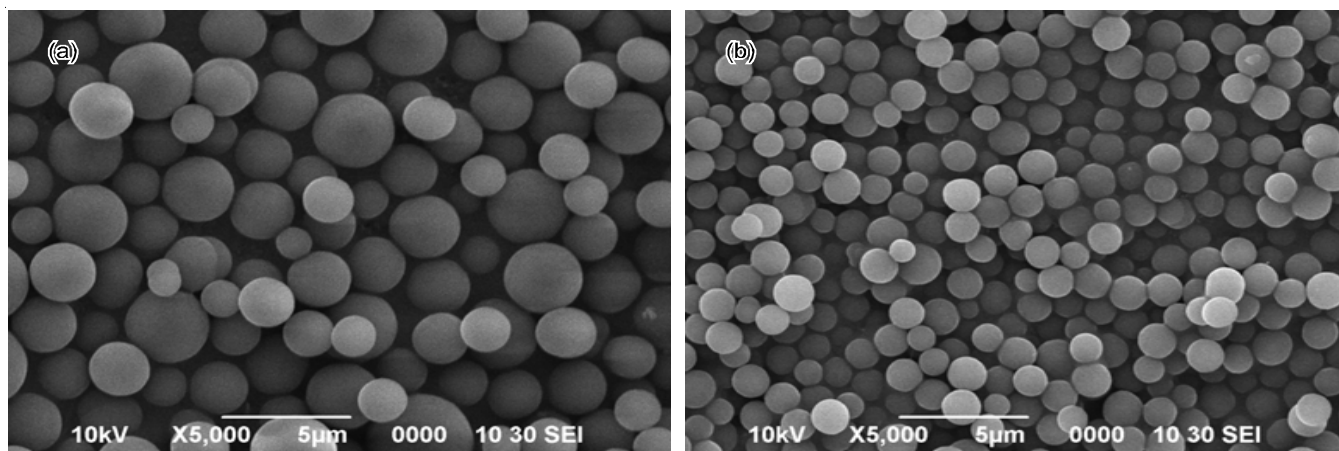


Fig. 2. SEM of NIP (a) and MIP (b)

Brunauer-Emmett-Teller of MIP and NIP: The specific surface areas, pore diameters and pore volumes of MIP and NIP are shown in Table-3. The results reported that all the parameters such as specific surface area, average pore diameter and pore volume of MIP were greater than that of NIP. This indicated that the presence of template during the synthesis of MIP has created a cavity. The presence of template has avoided the shrinkage of the pores effectively during the polymerization. This may be the main reason that MIP had a greater pore size and pore volume than NIP. The presence of template during polymerization of MIP has also produced a complementary spatial structure for the selective recognition of the target molecule.

Properties	Magnitude MIP	Magnitude NIP
Surface area (m ² /g)	10.1040	6.5060
Average pore radius (Å)	4.7236	1.1544
Total pore volume (cc/g)	3.3860	2.5750

Batch binding studies: The re-binding property of the polymers was evaluated using batch binding experiment. It is clear from Fig. 4a that the binding efficiency was very high at 90 min. The results from binding experiment showed that all imprinted polymers have good re-binding efficiency. But among all the three polymers, MIP3 has shown higher efficiency as compared to MIP1 and MIP2. This may be due to the higher number of complimentary binding sites in MIP3. From Fig. 4b, it is also clear that the binding efficiency of MIP is always higher as compared to NIP. This may be due to the absence of complementarily binding site in NIP. The template binding by NIP can be described with the existence of non-selective adsorption because of physical adsorption and may be accidental interactions of the template molecules with functional groups in the polymer matrix. In contrast, MIP rebinded much more efficiently than that of NIP since MIP had created specific recognition sites in imprinting cavities.

Effect of initial concentration: The initial concentration of MIP is an important factor which induced the process of adsorption. The batch study for effect of an initial concentration of thymol was carried out from 10 ppm to 30 ppm at constant conditions of agitation speed 250 rpm, pH 7, contact time 90

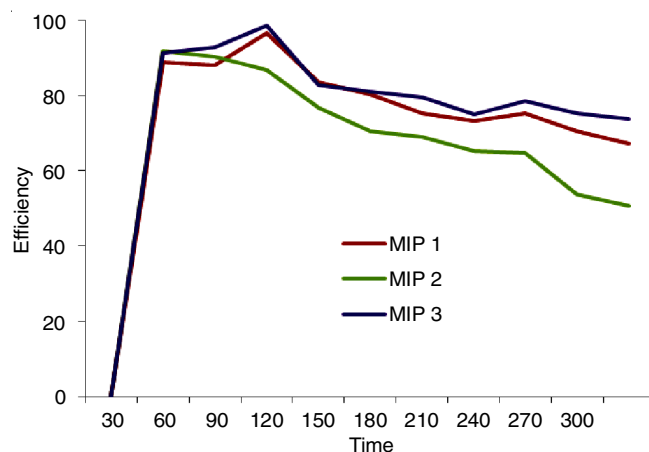


Fig. 4(a). Binding efficiencies of MIPS (MIP1, MIP2, MIP3)

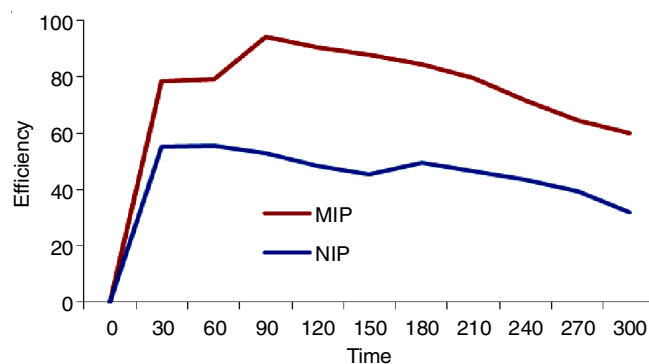


Fig. 4(b). Binding efficiencies of MIP vs. NIP

min and MIP dose 300 mg. The adsorption increases upto 20 ppm and further increase in concentration have shown that the process of adsorption have slightly decreases (Fig. 5). The decrease of adsorption is possibly because of the saturation of active adsorption sites on the MIP. The maximum adsorption (94 %) was detected at a concentration of 20 ppm. At low concentration, thymol was not sufficient to saturate the specific binding sites. Therefore, there was an increasing trend of adsorption observed until all the binding sites have been saturated with the template.

Effect of pH: The influence of pH on the binding of imprinted polymer was observed at different values (pH 2, 5, 7, 9, 12). The results (Fig. 6) clearly indicated that the adsorption capacity is higher at pH 7. The results displayed that at low

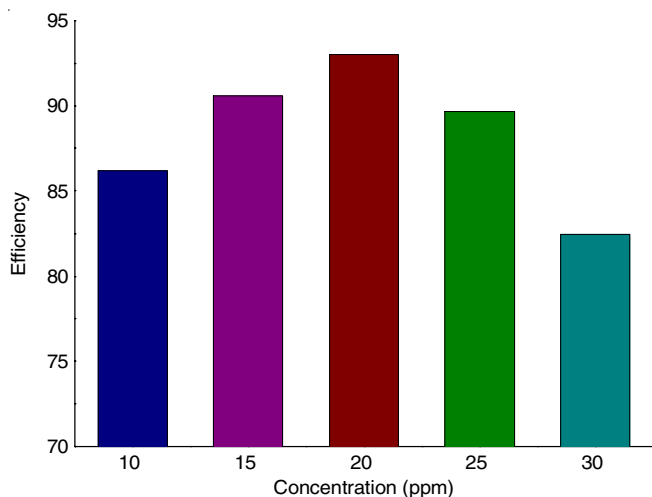


Fig. 5. Effect of initial concentration on the binding efficiency

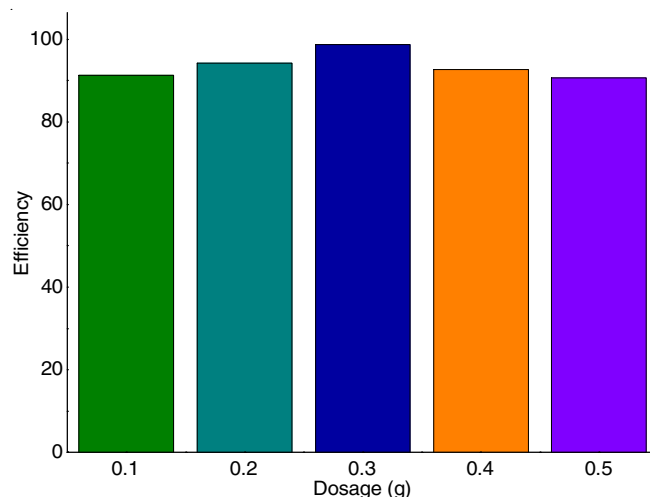


Fig. 7. Effect of polymer dosage on the binding efficiency

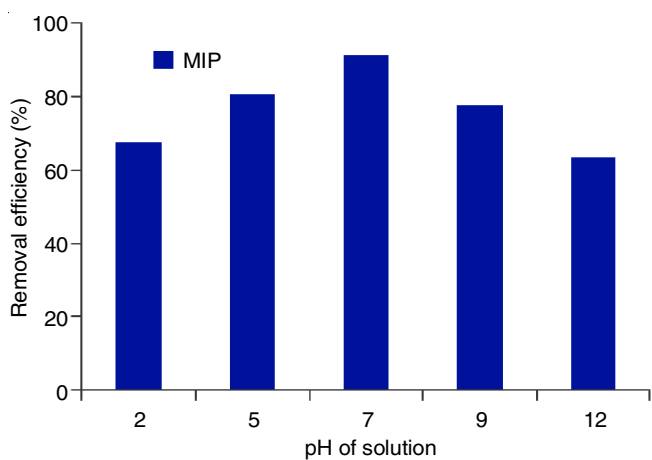


Fig. 6. Effect of pH on the binding efficiency

pH (acidic range) and at high pH (basic range), the adsorption capacity is low as compared to the observed at pH 7. This indicated that the functionality of template has been altered due to the change in the pH of template solution. This also indicated that at low pH (acidic) and at higher pH (basic) template have modified functionalities not complementarily with the sites available in the cavities of polymer. It has been reported that in most of the cases neutral pH is the best condition for the formation of hydrogen bonding between functional groups of binding sites and template molecules [29,34].

Effect of polymer dosage: The dependence of dosage on the binding efficiency of thymol was studied by varying the amount of MIP from 100 mg to 500 mg. Fig. 7 displayed that the removal efficiency of thymol has increased with an increase in the mass of polymer upto a limit of 300 mg. This is due to the fact that an increased dosage of MIP leads an increase in the binding sites available for the sorption of thymol onto the MIP's surface [35]. But after further increase in polymer dosage, a decrease in adsorption has been observed. This may be due to the aggregation of polymer particle in the template solution and in turn have reduced the accessibility towards the available binding sites.

Effect of change in agitation rate: Changes in the speed of agitation on the adsorption process were studied in the range of 100-300 rpm, while the other parameters were kept constant

(298 K, 20 ppm, 90 min, 300 mg and pH 7). Fig. 8 shows that the adsorption of thymol on MIP was increased from 100 rpm (69 %) to 250 rpm (92 %) with an increase of agitation rate, further increase in agitation rate decrease the extent of adsorption. The increase in the uptake of thymol by MIP was probably due to the decline in the diffused layer thickness of MIP surface.

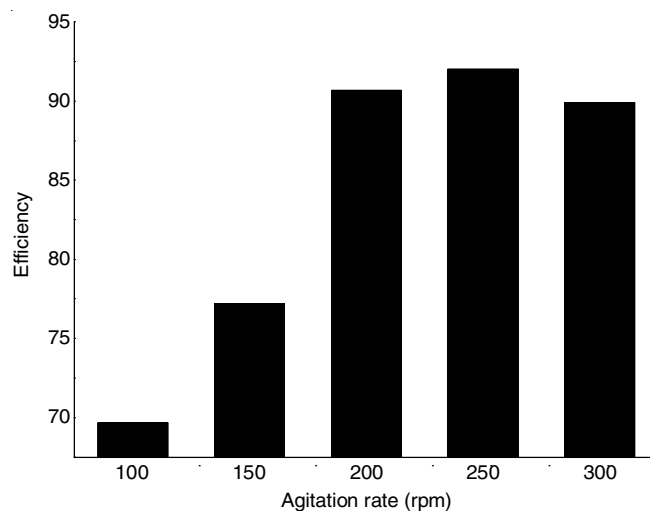


Fig. 8. Effect of agitation rate on binding efficiency

Selectivity of MIP: Different factors such as particle size of material and the shape of recognition sites will affect the ability of polymers in selectivity recognition [36]. Therefore, thymol and its structural analogue (gallic acid) were tested together to evaluate the selectivity of imprinted polymer. Distribution coefficient (K_D), selectivity coefficient (α) and relative selectivity coefficient (β) values of MIP and NIP for both templates are listed in Table-4. The binding amount of thymol on MIP is higher than gallic acid, which means that the template molecule has higher affinity than its analogue for imprinted polymer. Gallic acid binding to MIP is due to the non-selective and non-specific interactions. The high binding ability of MIP towards the thymol is derived mainly from the existence of cavities complementary both in shape and functional groups with thymol. Gallic acid had a less chance to interact with the MIP. The binding capacity of NIP for the substrates was owing to physical adsor-

TABLE-5
EXTRACTION EFFICIENCY OF MIP AND NIP IN DIFFERENT SAMPLES CONTAINING THYMOL

Samples	MIP 3				NIP		
	Amount of THY added (µg/mL)	Amount of THY found (µg/mL)	Recovery (%)	RSD (%)	Amount of THY found (µg/mL)	Recovery (%)	RSD (%)
Blood serum	20	16.8	84	0.31	10	50	0.54
River water	20	19.6	98	0.15	14	70	0.33

TABLE-4
SELECTIVITY DATA OF MIP AND NIP

Templates	K _D (MIP)	K _D (NIP)	α MIP	α NIP	β
Thymol	7.08549	6.02404	1.302	0.362	3.59
Gallic acid	5.440199	16.64076			

ption, which was non-specific adsorption and had less selectivity. As shown in Table-4, the relative selectivity coefficient (3.59) between thymol and gallic acid is very significant.

Extraction/removal of thymol in environmental and biological samples: In this study, thymol was successfully extracted from the spiked blood serum and river water samples. The results showed that a considerable amount of thymol was extracted from the spiked samples (Table-5).

Conclusion

In this study, molecular imprinted polymers (MIPs) were prepared by using non-covalent imprinting approach by precipitation polymerization. The morphological and adsorption features of polymers have been investigated. MIP had high adsorption capacity, selectivity and good site availability for thymol. SEM morphologies have displayed spherical microsphere polymer particles. This was achieved because of precipitation polymerization. It was confirmed that the shape and size of the template as well as the strength of interaction between the target molecule and binding sites to determine MIP selectivity. The MIPs were successfully applied for extraction/removal of thymol from spiked human serum and river water.

CONFLICT OF INTEREST

The authors declare that there is no conflict of interests regarding the publication of this article.

REFERENCES

- British Pharmacopoeia on CD-ROM, Version 5, Copyright by System Simulation Ltd., The Stationery Office Ltd.: London, vol. 1, edn 3, p. 1288 (1998).
- N. Szentandrassy, P. Szentesi, J. Magyar, P.P. Nánási and L. Csernoch, *BMC Pharmacol.*, **3**, 9 (2003); <https://doi.org/10.1186/1471-2210-3-9>.
- P.M. Dewick, *Medicinal Natural Products*, Wiley: Chichester, edn 2, p. 180 (2002).
- N. Szentandrassy, Ph.D. Thesis, University of Debrecen (2003).
- V. Solinas, C. Gessa and L.F. Delitala, *J. Chromatogr. A*, **219**, 332 (1981); [https://doi.org/10.1016/S0021-9673\(00\)87947-9](https://doi.org/10.1016/S0021-9673(00)87947-9).
- M.D. Rafiul, S.H. Ansari, N. Abdulkalam and J.N. Kamran, *Int. J. Pharm. Pharm. Sci.*, **4**, 478 (2012).
- M. Shekarchi, M. Khanavi, N. Adib, M. Amri and H. Hajimehdipoor, *Pharmacogn. Mag.*, **6**, 154 (2010); <https://doi.org/10.4103/0973-1296.66927>.
- R.D. Thompson and M. Carlson, *J. Pharm. Biomed. Anal.*, **7**, 1199 (1989); [https://doi.org/10.1016/0731-7085\(89\)80055-X](https://doi.org/10.1016/0731-7085(89)80055-X).
- L. Ji, Y.Y. Wang, Y. Tong, X.D. Li, X.F. Feng, L.Q. Hang and G.P. Zhou, *Zhongguo Zhongyao Zazhi*, **29**, 1030 (2004).
- K. Li, J. Yuan and W. Su, *Yakugaku Zasshi*, **126**, 1185 (2006); <https://doi.org/10.1248/yakushi.126.1185>.
- H. Gao, W. Cao, Y. Liang, N. Cheng, B. Wang and J. Zheng, *Chromatographia*, **72**, 361 (2010); <https://doi.org/10.1365/s10337-010-1628-4>.
- C. Kohlert, G. Abel, E. Schmid and M. Veit, *J. Chromatogr. B Analyt. Technol. Biomed. Life Sci.*, **767**, 11 (2002); [https://doi.org/10.1016/S0378-4347\(01\)00518-7](https://doi.org/10.1016/S0378-4347(01)00518-7).
- T.-T. Nhu-Trang, H. Casabianca and M.-F. Grenier-Loustalot, *J. Chromatogr. A*, **1142**, 219 (2006); <https://doi.org/10.1016/j.chroma.2006.07.088>.
- M.W. Noall, V. Knight, W.W. Hargrove and B.W. Elledge, *Anal. Biochem.*, **69**, 10 (1975); [https://doi.org/10.1016/0003-2697\(75\)90559-X](https://doi.org/10.1016/0003-2697(75)90559-X).
- A. Tsigouri, M. Passaloglou-Katrali and O. Sabatakou, *Acta Aliment.*, **37**, 181 (2008); <https://doi.org/10.1556/AALim.2007.0032>.
- R. Badertscher, V. Kilchenmann, A. Liniger and P. Gallmann, *J. ApiProd. ApiMed. Sci.*, **2**, 87 (2010); <https://doi.org/10.3896/IBRA.4.02.3.01>.
- G.M.L. Fiori, P.S. Bonato, M.P.M. Pereira, S.H.T. Contini and A.M.S. Pereira, *J. Braz. Chem. Soc.*, **24**, 837 (2013); <https://doi.org/10.5935/0103-5053.20130109>.
- O.W. Lau, S.F. Luk and W.C. Wong, *Analyst*, **113**, 865 (1988); <https://doi.org/10.1039/an9881300865>.
- U.I.S. Al-Neaimy, *J. Edu. Sci. (Iraq)*, **22**, 125 (2009).
- M.S. Al-Enizzi, T.N. Al-Sabha and Th. S. A I-Ghabsha, *Jordan J. Chem.*, **7**, 87 (2012).
- M.A. Korany, A.A.S. El-Din and N.A. Abael-salam, *Anal. Lett.*, **17**, 483 (1984); <https://doi.org/10.1080/00032718408065296>.
- L. Fibranz, M.I. Blake and C.E. Miller, *J. Am. Pharm. Assoc.*, **47**, 133 (1958); <https://doi.org/10.1002/jps.3030470215>.
- L.I.A. Basha, M.S. Rashed and H.Y. Aboul-Enein, *J. Liq. Chromatogr.*, **18**, 105 (1995); <https://doi.org/10.1080/10826079508009224>.
- A. Bazytko and H. Strzelecka, *Chromatographia*, **52**, 112 (2000); <https://doi.org/10.1007/BF02490803>.
- M.Q. Al-Abachi and H.S. Al-Ward, *J. Baghdad Sci.*, **9**, 302 (2012); <https://doi.org/10.21123/bsj.9.2.302-310>.
- G. Wulff and A. Sarhan, *Angew. Chem. Int. Ed. Engl.*, **11**, 341 (1972).
- L. Wang, W. Fu, Y. Shen, H. Tan and H. Xu, *Molecules*, **22**, 508 (2017); <https://doi.org/10.3390/molecules22040508>.
- N.A. Yusof, N.D. Zakaria, N.A.M. Maamor, A.H. Abdullah and M.J. Haron, *Int. J. Mol. Sci.*, **14**, 3993 (2013); <https://doi.org/10.3390/ijms14023993>.
- M. Masoumi and M. Jahanshahi, *Adv. Polym. Technol.*, **35**, 221 (2015); <https://doi.org/10.1002/adv.21548>.
- M. Esfandyari-Manesh, M. Javanbakht, F. Atyabi, A. Badiei and R. Dinarvand, *J. Appl. Polym. Sci.*, **121**, 1118 (2011); <https://doi.org/10.1002/app.33812>.
- S.A. Bhawani, T.S. Sen and M.N.M. Ibrahim., *Chem. Cent. J.*, **12**, Article No. 19 (2018); <https://doi.org/10.1186/s13065-018-0392-7>.
- A.L.J. Chow and S.A. Bhawani, *Int. J. Polym. Sci.*, **2016**, Article ID 2418915 (2016); <https://doi.org/10.1155/2016/2418915>.
- R.M. Roland and S.A. Bhawani, *J. Anal. Methods Chem.*, **2016**, Article 5671507 (2016); <https://doi.org/10.1155/2016/5671507>.
- M. Esfandyari-Manesh, M. Javanbakht, F. Atyabi and R. Dinarvand, *J. Appl. Polym. Sci.*, **125**, 1804 (2012); <https://doi.org/10.1002/app.36288>.
- A.B. Dekhil, Y. Hannachi, A. Ghorbel and T. Boubaker, *J. Environ. Sci. Technol.*, **4**, 520 (2011); <https://doi.org/10.3923/jest.2011.520.533>.
- H. Zeng, Y. Wang, X. Liu, J. Kong and C. Nie, *Talanta*, **93**, 172 (2012); <https://doi.org/10.1016/j.talanta.2012.02.008>.